Biophysical Chemistry 184 (2013) 1–7

Contents lists available at ScienceDirect

Biophysical Chemistry

journal homepage: http://www.elsevier.com/locate/biophyschem

Precise quantification of transcription factors in a surface-based single-molecule assay

Kristin S. Grußmayer, Tanja Ehrhard, Konstantinos Lymperopoulos *, Dirk-Peter Herten *

CellNetworks Cluster and Institute for Physical Chemistry, Heidelberg University, Im Neuenheimer Feld 267, 69120 Heidelberg, Germany

HIGHLIGHTS

- Single-molecule based assay for quantitative detection of transcription factors
- Improved quantitative modeling of data from single-molecule experiments
- Immobilized assay format reaches higher sensitivity than solution based approach.

GRAPHICAL ABSTRACT

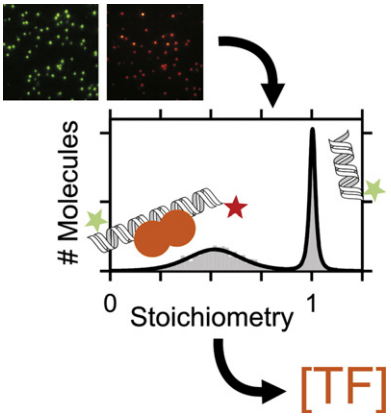

ARTICLE INFO

Article history:
Received 20 June 2013
Received in revised form 30 July 2013
Accepted 31 July 2013
Available online 15 August 2013

Keywords:
Biosensor
Quantitative detection
Transcription factor
Single-molecule study
Surface immobilization

ABSTRACT

Biosensors have recognized a rapid development the last years in both industry and science. Recently, a single-molecule assay based on alternating laser excitation has been established for the quantitative detection of transcription factors. These proteins specifically recognize and bind DNA and play an important role in controlling gene expression. We implemented this assay format on a total internal reflection fluorescence microscope to detect transcription factors with immobilized single-molecule DNA biosensors. We quantify transcription factors via colocalization of the two halves of their binding site with immobilized single molecules of a two-color DNA biosensor. We could detect a model transcription factor, the bacterial lactose repressor, at different concentrations down to 150 pM. We found that robust modeling of stoichiometry derived TIRF data is achieved with Student's t-distributions and nonlinear least-squares estimation with weights equal to the inverse of the expected number of bin entries. This significantly improved transcription factor concentration estimates with respect to distribution modeling with Gaussians without adding notable computational effort. The proposed model may enhance the precision of other single-molecule assays quantifying molecular distributions. Our measurements reliably confirm that the immobilized biosensor format is more sensitive than a previously published solution based approach.

1. Introduction

Biosensors have recognized a rapid development the last years in both industry and science. Although in the past decade the focus was

* Corresponding authors. Tel.: +49 6221 54 51 220; fax: +49 6221 54 51 444.
E-mail addresses: klymperopoulos1@gmail.com (K. Lymperopoulos), dirk.herten@bioquant.uni-heidelberg.de (D.-P. Herten).

0301-4622/$ – see front matter © 2013 Elsevier B.V. All rights reserved.
http://dx.doi.org/10.1016/j.bpc.2013.07.015

on automation, in recent years it has shifted to miniaturization trying to integrate the detection of biomaterials with nanostructures [1]. An important parameter of miniaturization is whether the biosensor is amenable to surface-based immobilization. The new generation of biosensors must not only provide a qualitative answer on the presence of the analyte in question, but must also be capable of quantitative determination. Here, we set out to use immobilized DNA biosensors to quantify transcription factors (TFs), proteins that specifically recognize and bind DNA. TFs are pivotal molecules that control gene expression and their dysregulated profile is involved in numerous cancer types and diseases [2–4]. For this reason, their rapid and ultrasensitive detection is of essence in molecular diagnostics [5]. Long-established biochemical methods such as DNAse footprinting, electrophoretic mobility shift assays (EMSAs) and western blotting provide valuable information on characterizing TFs but are time-consuming, require large amounts of sample, and are at best semi-quantitative [6]. Enzyme-linked immunosorbent assays (ELISAs) and recent techniques such as the proximity-based ligation assay offer sensitive detection [6,7]. Their need for signal amplification renders them ill-suited for fast diagnosis, although their immobilization scheme offers a notable advantage for multiplexing and high-throughput capabilities.

Recently, TF detection with a single-molecule DNA biosensor was reported based on TF-induced coincidence of fluorescently labeled DNAs [8]. TF sensing of catabolite activator protein (CAP) and lac repressor (lacR; aka lacI), both involved in the regulation of bacterial lactose metabolism [9,10], was quantitatively investigated in solution using alternating-laser excitation (ALEX) and the robustness of the assay in cell extracts was demonstrated. Additionally, it was shown that in principle this assay also works with immobilized biosensors on surfaces. However, in order for the single-molecule DNA biosensor to be fully utilized in the immobilized scheme a thorough quantification and optimization is needed. Here, we continue the work published by Lymperopoulos et al. by precisely quantifying the fraction of lacR bound DNA using immobilized biosensors. We present an improved model for accurately describing the molecular distributions in stoichiometry-based single molecule experiments and adapted the established theoretical description of the biosensor response to surface-based measurements.

2. Results and discussion

2.1. TF sensing with DNA biosensors

The biosensors were constructed as described in ref. [8]. In brief, the biosensor comprises the TF–DNA target site split into two parts. These DNA fragments, termed half-sites (H), have short, complementary single stranded (ss) overhangs. In our assay, one half-site ($H1^G$) is labeled with a green fluorophore and biotinylated for single-molecule immobilization via biotin–neutravidin on a BSA passivated surface (see Materials and methods). The other half-site ($H2^R$) is labeled with a spectrally distinct red fluorophore and supplied in solution along with the TF (Fig. 1a). The tendency of the DNA fragments to associate is designed to be low such that in the absence of TF the fraction of annealed DNA half-sites is insignificant (Fig. 1c, bottom, Fig. 2a, bottom and Supporting Information Fig. S2a). We investigate lacR with a biosensor that has only 6 bases ss overhang and use low nanomolar concentrations of half-site $H2^R$ to satisfy this requirement. When the protein is present in the reaction mixture, it will selectively bind to the assembled binding site and drive the association of $H1^G$ and $H2^R$ (see Fig. 1b and c, top). We confirmed that lacR does not bind to one half-site alone with ensemble EMSAs (see Supporting Information Fig. S3). Protein-dependent colocalization of $H1^G$ and $H2^R$ is detected using ALEX on a total internal reflection fluorescence (TIRF) microscope. The fluorescently labeled half-sites of the single-molecule biosensor are sampled by alternating excitation with green and red laser lights. For each molecule in the green detection channel the average apparent Förster resonance energy transfer (FRET) efficiency (E^*) and stoichiometry (S) are calculated excluding unspecifically adsorbed $H2^R$ from the analysis (see Materials and methods). The assay readout does not require a change in FRET efficiency for TF sensing, but FRET may be used as an additional parameter for sensor encoding. Therefore, the S-based detection scheme allows a free choice of dye positions along the DNA, here at the respective ends of the half-sites to avoid perturbation of TF–DNA binding [8]. The interfluorophore distance is 40 base pairs (~13.6 nm) for the assembled half-sites of the lacR biosensor, corresponding to more than twice the Förster radius $R_0 = 6.2$Å for the Cy3B–Atto647N dye pair, so FRET can be neglected in our experiments [11]. With $E^* = 0$ in the TF bound and unbound sensor configuration, S reports on the molecular stoichiometry. The population with stoichiometry around S ~ 0.55 (mid S, $H1^G$ colocalized with $H2^R$, Fig. 2a) contains the TF bound to both half-sites and the population with S ~ 1 represents the unbound biosensor (high S, $H1^G$ only). An increase in lacR bound biosensor with increasing lacR concentration is thus indicated by a gain in the relative area of the mid S population. The mid S population is much broader than the high S population due to the contribution of two fluorescent signals and because of additional intensity variations of the red dye Atto647N [11,12]. The fraction of TF bound DNAs is determined by estimating the mixing proportion of the mid S population using a bimodal fit model (Fig. 2a,b).

2.2. Improved model for stoichiometry distributions

An important aspect of accurately quantifying TFs, i.e. measuring the fraction of colocalized half-sites, is the use of a probability distribution function (PDF) that describes the two populations' (bound and unbound biosensors) best. Therefore, we carefully examined different PDFs and parameter estimation approaches. We tested maximum likelihood estimation(MLE) and non-linear least-squares (NLS) parameter estimation with different weights and compared Gaussian and three parameter Student's t distributions (see Materials and methods and Supporting Information) [13,14]. It should be noted that the Student's t distribution comprises the Gaussian distribution as a limiting case and was used before to achieve robust modeling of biological data sets [15,16]. We combined data from ~20 movies of different fields of view in one histogram with appropriate binning to assess the TF bound fraction for one experiment. The histogram was then modeled using the approaches described above. Fit quality was judged by examination of the residuals and by calculation of Pearson's $\chi^2_{\mathrm{red}} = \frac{1}{\mathrm{d.\ o.\ f.}} \sum_i \frac{(O_i - E_i)^2}{E_i}$ (red = reduced, d.o.f. = number of degrees of freedom, O_i are the observed counts and E_i are the expected counts). In addition, we performed a χ^2-goodness-of-fit test with the null hypothesis that the data are a random sample from the respective PDF (see Supporting Information) [13,14].

Both NLS estimation with weights equal to the inverse of the expected number of bin entries and MLE using a linear combination of two Student's t-distributions performed best [13]. We selected the NLS estimation to evaluate all the data due to computational speed. A comparison of the chosen fitting approach with the commonly applied ordinary non-linear least-squares (ONLS) estimation using a linear combination of two Gaussians (Fig. 2b) illustrates that the latter misses the tails of the narrow high S population. Only in the case of the Student's t-distributions χ^2_{red} is close to one and the null hypothesis of the χ^2-goodness-of-fit test cannot be rejected at the 5% significance level (see Supporting Information). Fig. 2c compares the Gaussian with the Student's t model based on the resulting relative deviation of the DNA colocalization. It is evident that the Gaussian model shows a systematic positive bias of up to 200% with respect to the Student's t model. In more than 50% of the experiments the TF bound fraction is overestimated by at least 10–20%. We also found that the bias becomes more significant for low TF concentrations (see Supporting Information Fig. S1).

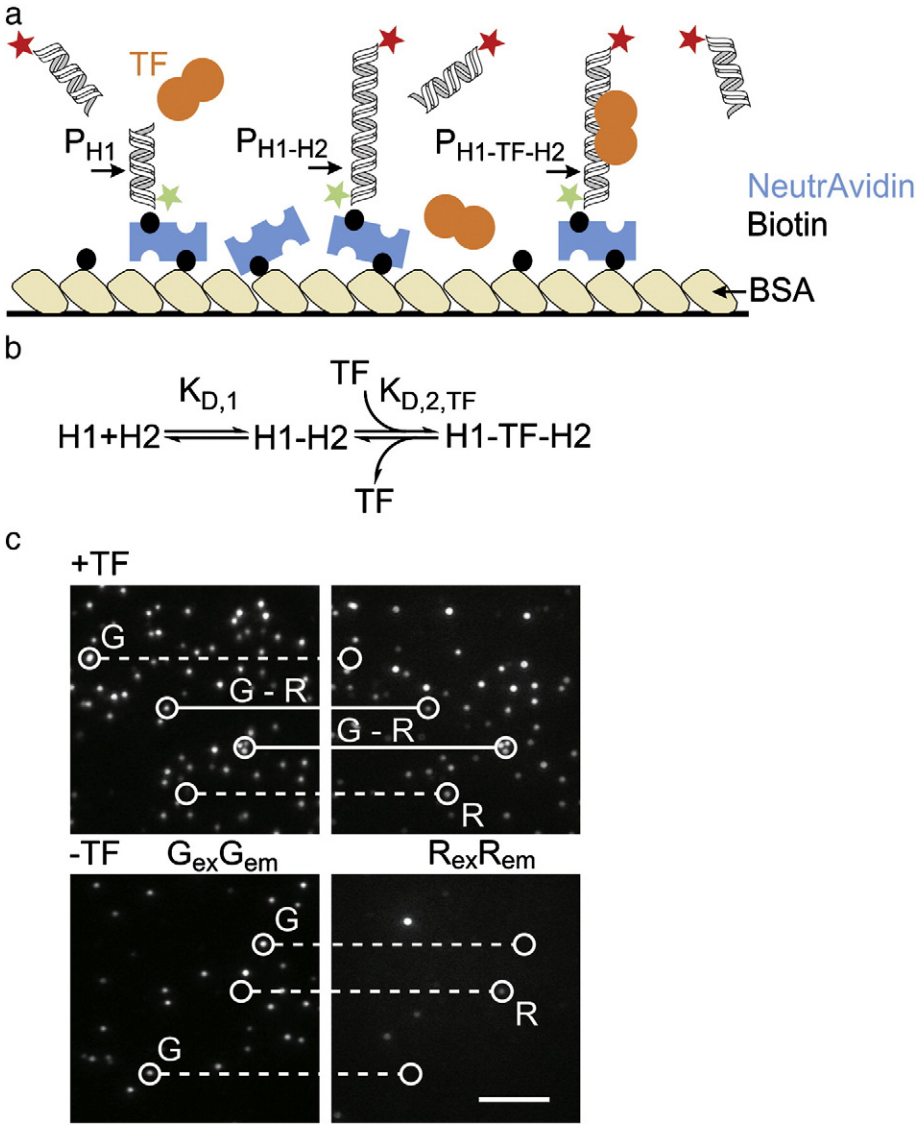

Fig. 1. Surface immobilized TF biosensor based on DNA colocalization. a) The biosensor consists of two DNA half-sites H, each labeled with a green and a red fluorophore respectively. TF binding drives formation of a stable complex (see text for details). b) The model describing the biosensor principle consists of half-site association (K_{D1}) and TF binding to the assembled target site (K_{D2}). c) TIRF images show spots of immobilized $H1^G$ in the green detection channel (left) that colocalize with red spots (right) of $H2^R$ in presence of TF (G-R, upper images). Without TF, primarily green-only spots (G) occur along with few spots of unspecifically bound red half-sites (R, lower images). Scale bar is 5 μm.

2.3. Theoretical description of surface-immobilized biosensor response

Analysis of the histograms leads to the determination of the TF bound fraction depending on the experimental conditions. We adapted the previously applied model of two coupled equilibria, one for half-site association with dissociation constant K_{D1} and a second for TF binding to the assembled target site with K_{D2}, to describe measurements with immobilized single half-sites (Fig. 1b) [8,17,18]. The notation is changed from concentrations of species involving $H1^G$ ($[H1^G]$, $[H1^G - H2^R]$, $[H1^G - TF - H2^R]$) to probabilities of the corresponding equilibrium states of the immobilized probe (P_{H1^G}, $P_{H1^G-H2^R}$, $P_{H1^G-TF-H2^R}$, see Fig. 1a). In addition, we assume that the concentrations of TF and $H2^R$ in solution remain constant because they are present in large molar excess over the surface bound half-site. The TF bound fraction equals the probability to be in the TF bound state $P_{H1\text{-}TF\text{-}H2}$ and depends on K_{D1}, K_{D2}, $[H2^R]$ and [TF]. In turn, the unknown concentration of TF can be calculated from the experimentally determined bound fraction at specified $[H2^R]$ provided the dissociation constants are known (see Materials and methods).

2.4. Comparison of experimental lacr detection with the theoretical biosensor model predictions

In the experiments, we titrated 0–300 nM active lacR along with 1 nM or 5 nM half-site $H2^R$ on a surface with immobilized half-site $H1^G$. In addition, we investigated the effect of the change of incubation temperature on the sensitivity and population distribution. We varied the temperature from 14 °C to room temperature (RT) for 1 nM $H2^R$ in search of optimized experimental conditions. To compare the normalized DNA colocalization extracted from our measurements with the predictions of the model, we used NLS regression with weights equal to the experimental error.

For the analysis with 5 nM half-site, we kept the half-site concentration constant ($[H2^R = 5\ nM]$) and fitted the remaining model parameters (Fig. 3a). The estimated dissociation constant for half-site binding was $K_{D1,14\ °C} = 240$ nM, a value that agrees well with ensemble thermophoresis measurements (see Supporting Information). The estimate is slightly lower than $K_{D1,14\ °C} = 300$ nM for the catabolite activator protein (CAP) biosensor under the same conditions [8]. This was

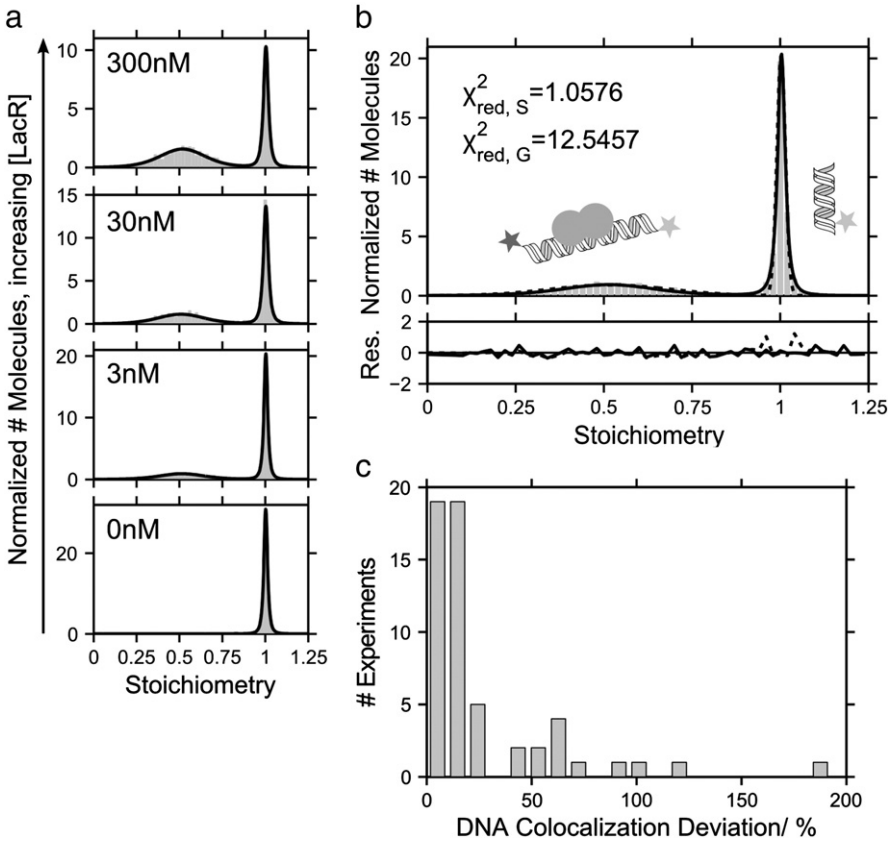

Fig. 2. Single-molecule sensing of lacR with an immobilized DNA biosensor. a) Normalized stoichiometry distributions of immobilized $H1^G$ with 1 nM $H2^R$ as a function of lacR concentration at RT. The high S (S ~ 1.0) population represents $H1^G$ (green-only) whereas the mid S (S ~ 0.55) population (colocalized green and red fluorescence) comprises the complex $H1^G$-LacR-$H2^R$. b) Normalized stoichiometry distribution at 3 nM lacR concentration from a) for comparison of model fits using a linear combination of two Student's t-distributions (subscript S, solid line) and two Gaussians (subscript G, dashed line). c) Deviation of the DNA colocalization (DC) determined by modeling two Gaussians with respect to the result obtained with two Student's t-distributions DCDev. $= \frac{DC_G - DC_S}{DC_S}$.

expected since the biosensor used in this work has a higher GC content in the single-stranded overhangs of same length. The association of lacR with its DNA target site is described by $K_{D2,14\ °C} = 12$ pM, in good agreement with previous affinity measurements K_{D2} ~ 10 pM at comparable ionic strengths [19–22]. The surface bound assay is very sensitive in the low nM range and we detected down to 150 pM active lacR with 5 nM and 1 nM half-site $H2^R$ in the solution upon incubation at 14 °C (see Supporting information Fig. S2). The measurements with 1 nM half-site can be described by the theoretical model with $K_{D1,14\ °C} = 240$ nM, $K_{D2,14\ °C} = 12$ pM and [$H2^R = 1$ nM](Fig. 3b).

An additional set of experiments was conducted with 1 nM half-site $H2^R$ and incubation at room temperature. The data series is well described by $K_{D2,RT} = 6$ pM for protein-DNA interaction and estimation of the half-site dissociation constant resulted in $K_{D1,RT}$ ~ 580 nM (Fig. 3c). The binding of lacR to its operator was previously found to tighten moderately with temperature, i.e. K_{D2} decreases [22,23]. In turn, we expect a reduction in $H1^G - H2^R$ affinity, i.e. an increase of K_{D1}, from DNA thermodynamics theory [24]. The combined effect results in a biosensor response curve that is marginally shifted to higher TF concentrations at room temperature compared to 14 °C for the lac repressor (Fig. 3d). The response of this biosensor is essentially unaltered by the applied change in temperature.

In general, sensor sensitivity may be altered by changes in half-site concentration, K_{D1} (e.g. modification of the single-stranded overhangs) and K_{D2} (e.g. mutations in the TF binding site) [8,17]. In case of surface-immobilized TF, raising [$H2^R$] is limited to ~10 nM due to unspecific adsorption on the surface and a high background signal. Working with higher concentrations of $H2^R$ might be feasible by quantifying false positives using the localization based method established by Trabesinger et al. or zero-mode waveguides to further reduce background [25,26]. In our experiments, a five-fold rise in [$H2^R$] results in an increased sensor responsiveness and earlier saturation of the measured curves. We validated the proof of principle measurement on the surface immobilized biosensor of ref [8] by systematic variation of the TF concentration and confirmed that it has a slightly increased sensitivity compared to the solution-based approach with equal amounts of 1 nM half-sites (see Fig. 3d) [8]. Many eukaryotic TFs have higher K_{D2} than the lacR, so this should be of advantage [4,27–29].

3. Conclusion

In conclusion, we have quantitatively characterized surface-based sensing of lacR with an immobilized two-color DNA biosensor. We could detect the model TF at different concentrations down to 150 pM in accordance with ref. [8]. However, we found that distribution modeling with Gaussians systematically overestimates the TF bound fraction especially at low TF concentrations. This is of particular interest as it can significantly influence the determination of the K_D of TF binding. We show that a more robust modeling of stoichiometry derived TIRF data is achieved with Student's t-distributions and NLS estimation with weights equal to the inverse of the expected number of bin entries. We could thereby improve TF concentration estimates without notable additional computational effort. We perceive that the proposed model may enhance the precision of other single-molecule assays quantifying molecular distributions.

In accordance with previous reports, our experiments together with a theoretical description showed that the immobilized biosensor is slightly more sensitive for small TF concentrations than the solution based approach. Time-to-result is, in principle, only limited by the incubation time and could be reduced to a few minutes. These results

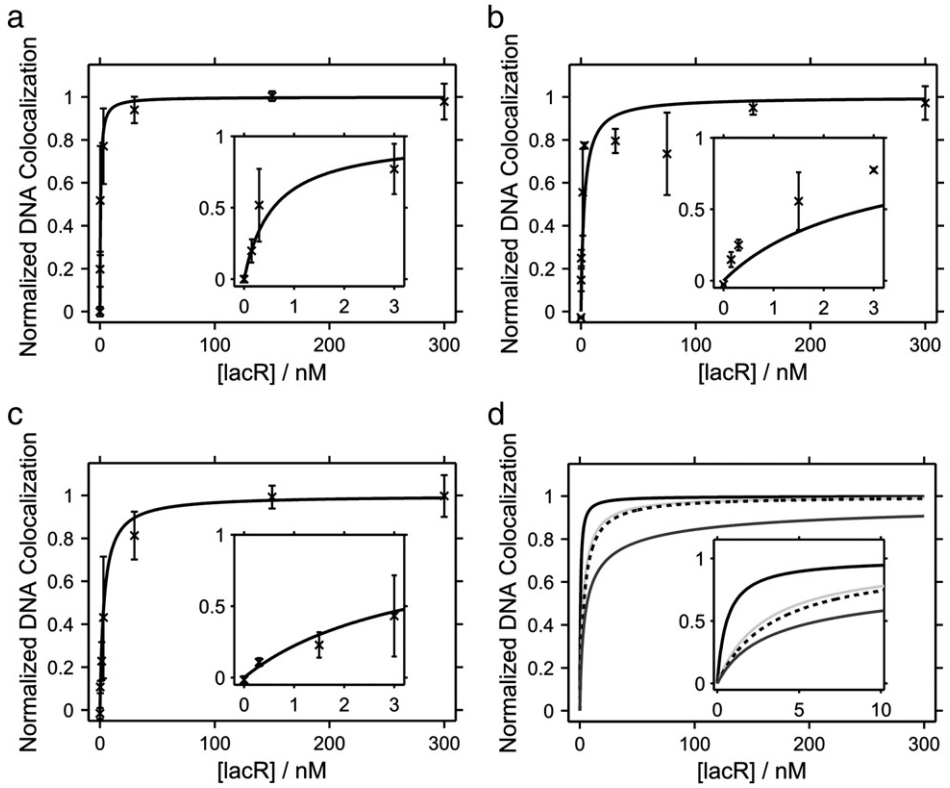

Fig. 3. Comparison of the modeled TF bound fraction and experimental TF quantification with immobilized half-sites. a), b),and c) Normalized DNA colocalization as a function of the active lacR concentration along with model predictions. The experimental uncertainty is given by the standard deviation. a) 5 nM, b) 1 nM and c) 1 nM $H2^R$ with incubation at a), b) 14 °C and c) RT. d) Model predictions of a) (solid black line), b) (solid light gray line), c) (dashed black line) and the model of the solution based approach of ref. [8] for 1 nM half-site each, supplied with the dissociation constants from a) (dark gray line).

reinforce the notion that the surface-based assay format provides good prospects for implementation in high-throughput applications for TF sensing based diagnostics.

4. Materials and methods

4.1. Materials

All chemicals (if not otherwise stated) were from Sigma-Aldrich.

4.2. Preparation of the DNA sensor

The oligonucleotides used were custom synthesized, (labeled) and high pressure liquid chromatography was purified from IBA GmbH, Göttingen, Germany and Sigma-Aldrich Chemie GmbH, Taufkirchen, Germany or Eurofins MWG Operon, Ebersberg, Germany. Sequences are given 5′ → 3′. lacR-A: (C6 Amine) TGG TGT GTG GAA TTG TGA, lacR-A-Cy3B = lacR-A labeled with N-hydroxy-succinimidyl ester (NHS) of Cy3B (GE Healthcare, Freiburg, Germany), lacR-B: GCG TAT AAC AAT TTC ACA CAG G, lacR-C: (C6 Amine) CCT GTG TGA AAT TGT T, lacR-C-Atto647N = lacR-C labeled with NHS ester of Atto647N (Atto-Tec GmbH, Siegen, Germany), lacR-D: ATACGCTCACAATTCCACA CACCA, lacR-D-Biotin = lacR-D with a biotin modification at the 3′-end. Oligonucleotides were hybridized in annealing buffer (20 mM Tris-HCl (pH 8.0), 500 mM NaCl, 1 mM EDTA) to form the half-sites (1 μM) by heating to 90 °C for 4 min and subsequent cooling to 25 °C (1 °C in 30s). Sensor naming convention: lacR AD (–Cy3B-Biotin) = $H1(^G)$ and lacR BC (–Atto647N) = $H2(^R)$.

$$\begin{aligned} H1\text{–}H2 = {} & 5'\text{—lacR—A–lacR—B—}3' \\ & 3'\text{—lacR—D–lacR—C—}5' \end{aligned}$$

4.3. Sample preparation

Binding reactions with lacR and ALEX-TIRF experiments were conducted in Lab-Tek chambered coverslides. The slides were cleaned twice with hydrofluoric acid (0.1 M) for 5 min, followed by 3 washes with 1× PBS and incubation with BSA and BSA–Biotin (20:1 ratio, 5 mg mL^{-1}) for 30 min. After incubation with 10 μg mL^{-1} neutravidin for 20 min, 10 pM of biotinylated $H1^G$ was immobilized on this coated surface. A mixture of 1 or 5 nM of H2-Atto647N and 0–300 nM active lacR in KG7 buffer (20 mM HEPES-NaOH (pH 7), 100 mM potassium-L-glutamate, 10 mM $MgCl_2$, 1 mM DTT, 0.1 mg mL^{-1} BSA, 1 mM MEA, 5% glycerol) was incubated in the Lab-Tek chamber at 14 °C or at room temperature for 30 min. Samples were immediately transferred to the microscope and imaged.

4.4. ALEX–TIRF experiments

ALEX-TIRFM data was acquired on a custom-built TIRFM setup consisting of a Zeiss Axioinvert 200 equipped with a 635 nm diode laser (TECRL-25G-635, World Star Tech, Toronto, Canada) and a 532 nm diode laser (TECGL-30, World Star Tech, Toronto, Canada) that were coupled into the microscope through the back port. An AOTF was alternating the laser excitation at the camera frame rate. Fluorescence was excited and collected with a microscope objective (Nikon CFI Apochromat TIRF 100× Oil, N.A. 1.49, Nikon Deutschland, Düsseldorf, immersion oil Nikon Immersol TM 518 F n = 1.518 (23 °C), Carl Zeiss, Jena) and isolated from excitation light by a dichroic mirror (z 532/633, AHF Analysentechnik, Tübingen, Germany). The detected light was focused through a rectangular aperture and filtered by a triple notch filter (488/532/631–640 nm, AHF Analysentechnik, Tübingen, Germany). The green and red detection channels were separated by a dichroic

mirror and further narrowed by bandpass filters (HQ 685/70 and HQ 585/60, AHF Analysentechnik, Tübingen, Germany) and focused on the two halves of the chip of a back-illuminated EMCCD camera (Andor iXonEM+ 897, Dublin, Ireland). A total of 20 individual movies of 2 s duration with an exposure time of 100 ms and laser excitation at ~50 W cm^{-2} were taken for each sample.

4.5. ALEX–TIRF data analysis

The average apparent FRET efficiency (E^*) [Eq. (1)] and the stoichiometry (S) [Eq. (2)] were calculated for all Cy3B-labeled molecules (R-G and G) over all frames before photobleaching, excluding the red only population (see Supporting information).

$$E^* = \frac{F^{R_{em}}_{G_{ex}}}{F^{G_{em}}_{G_{ex}} + F^{R_{em}}_{G_{ex}}} \tag{1}$$

$$S = \frac{F^{G_{em}}_{G_{ex}} + F^{R_{em}}_{G_{ex}}}{F^{G_{em}}_{G_{ex}} + F^{R_{em}}_{G_{ex}} + F^{R_{em}}_{R_{ex}}} \tag{2}$$

The data were inspected on E^*-S histograms and then combined and collapsed onto one-dimensional S histograms comprised of ~20 movies as shown in Fig. 2. The histograms were normalized to PDFs and fit with a linear superposition of two Student's t PDFs [Eq. (3)] to extract the bound fraction (F_B) in the low S population as described in detail in the main text and in the Supporting information. Only in absence of TF with 1 nM half-site fitting was not applicable with any of the models described above. Here, quantification of the TF bound fraction was achieved by dividing the number of green–red colocalized spots by the total number of green spots (see Supporting information Fig. S2).

$$\mathrm{PDF}\left(S\middle|F_B,\ \mu_{R\text{-}G},\lambda_{R\text{-}G},\nu_{R\text{-}G},\mu_G,\lambda_G,\nu_G\right) = F_B \mathrm{PDF}_{\text{Student's t}}\left(S\middle|\mu_{R\text{-}G},\lambda_{R\text{-}G},\nu_{R\text{-}G}\right) + (1-F_B)\mathrm{PDF}_{\text{Student's t}(S|\mu_G,\lambda_G,\nu_G)}. \tag{3}$$

With

$$\mathrm{PDF}_{\text{Student's t}}(S|\mu,\lambda,\nu) = \frac{\Gamma\left(\frac{\nu+1}{2}\right)}{\Gamma\left(\frac{\nu}{2}\right)}\left(\frac{\lambda}{\pi\nu}\right)^{\frac{1}{2}}\left[1+\frac{\lambda(S-\mu)^2}{\nu}\right]^{-\frac{\nu+1}{2}},$$

$\Gamma(x)$ $\int_0^\infty t^{x-1}e^{-t}dt$ the gamma function,
E(S) μ for $\nu > 1$ the expectation value,
var(S) $\frac{1}{\lambda}\frac{\nu}{\nu-2}$ for $\nu>2$ the variance.

The measured bound fraction at increasing lacR concentration was modeled by nonlinear least-squares regression as

$$F_{B,exp}\left(T,\left[H2^R\right]_{eq},[TF]_{eq}\right) = F_{B,0} + F_{B,exp,TF} = F_{B,0,theo} + c\,F_{B,theo}\left(K_{D1},K_{D2},\left[H2^R\right]_{eq},[TF]_{eq}\right) \tag{4}$$

with weights equal to the experimental error. The factor c accounts for a reduced bound fraction due to incomplete half-site hybridization, photobleaching of red labeled H2 and other species incapable of TF binding (see Supporting Information). $F_{B,0,theo}$ estimates the bound fraction in the absence of TF, i.e. false positives due to unspecifically bound $H2^R$ and includes minuscule half-site binding. All data analysis was performed on home-built software written in Matlab.

4.6. Model for surface bound measurements

To model the TF biosensor in case of surface immobilized H1, we state the definition of thermodynamic equilibrium (eq) for the two coupled reversible reactions (Fig. 2b), one for half-site association with dissociation constant K_{D1} [Eq. (5)] and a second for TF binding to the assembled target site with K_{D2} [Eq. (6)], in terms of the probabilities of the corresponding equilibrium states of the immobilized probe.

$$K_{D1} = \frac{P_{H1^G,eq}\left[H2^R\right]_{eq}}{P_{H1^G-H2^R,eq}} \tag{5}$$

$$K_{D2} = \frac{P_{H1^G-H2^R,eq}[TF]_{eq}}{P_{H1^G-TF-H2^R,eq}} \tag{6}$$

$$1 = P_{H1^G} + P_{H1^G-H2^R} + P_{H1^G-TF-H2^R} \tag{7}$$

We assume $[TF]_{eq} \approx [TF]_{total}$ and $[H2^R]_{eq} \approx [H2^R]_{total}$ due to large molar excess over the surface bound half-site. Neglecting the prebinding of half-sites without TF that is decribed by $P_{H1^G-H2^R,eq}$ because of the low nanomolar concentrations of $H2^R$ in solution and $K_{D1} >> K_{D2}$ (here $K_{D1} \geq 200$ nM, K_{D2} ~ 10 pM, see section Comparison of Experimental lacR Detection with the Theoretical Biosensor Model Predictions and ref. [8]), the colocalized DNA, i.e. the bound fraction $F_{B,theo}$ [Eq. (8)], equals the TF bound fraction $P_{H1^G-TF-H2^R,eq}$.

$$F_{B,theo}\left(K_{D1},K_{D2},\left[H2^R\right]_{eq},[TF]_{eq},\right) = \frac{\left[H2^R\right]_{eq}[TF]_{eq}}{[H2^R]_{eq}[TF]_{eq} + [H2^R]_{eq}K_{D2} + K_{D1}K_{D2}} \tag{8}$$

In case there is significant binding of DNA half-sites at [TF] = 0 in other biosensor experiments, $P_{H1^G-H2^R,eq}$ [Eq. (9)] may be added to the expression for $F_{B,theo}$.

$$P_{H1^G-H2^R,eq} = \frac{\left[H2^R\right]_{eq}K_{D2}}{[H2^R]_{eq}[TF]_{eq} + [H2^R]_{eq}K_{D2} + K_{D1}K_{D2}} \tag{9}$$

The model may readily be extended to consider TF oligomerization if applicable for the TF under investigation (see Supporting Information Fig. S4), as it is known that TFs can undergo oligomerization either before or after DNA binding. In our experiments we have no indication for lacR dimer–tetramer interconversion as more complex models did not improve the model fit to our data and native gel electrophoresis only showed one band for our protein preparation.

4.7. Purified lacR

LacR was prepared essentially as described in ref. [28] and ref. [29–31]. The activity was estimated by electrophoretic mobility shift assay to be ~30%, a common value for lacR preparations [32,33]. Size exclusion chromatography during purification of lacR and comparison with protein size standards indicate that lacR is present as a dimer in our preparations (see Supporting Information Fig. S5).

Acknowledgments

We gratefully acknowledge the support by Deutsche Forschungsgesellschaft (EXC81 and GRK1114). We also thank M. Kiehn and A. Kurz for the help with Matlab programming and I. Ganeva for the assistance with protein preparation. We are grateful to Dr. M. Brenowitz for kindly providing us with the plasmid for lacR expression.

Appendix A. Supplementary data

Supplementary data to this article can be found online at http://dx.doi.org/10.1016/j.bpc.2013.07.015.

References

[1] W. Demidov, Nanobiosensors and molecular diagnostics: a promising partnership, Expert Review of Molecular Diagnostics 4 (2004) 267–268.
[2] B. Vogelstein, D. Lane, A.J. Levine, Surfing the p53 network, Nature 408 (2000).
[3] G. Courtois, T.D. Gilmore, Mutations in the NF-κB signaling pathway: implications for human disease, Oncogene 25 (2006) 6831–6843.
[4] R. Eferl, E.F. Wagner, AP-1: a double-edged sword in tumorigenesis, Nature Reviews. Cancer 3 (2003) 859–868.
[5] K.E. Herold, A. Rasooly, Biosensors and molecular technologies for cancer diagnostics, Taylor & Francis, 2012.
[6] J. Sambrook, D.W. Russell, Molecular cloning: a laboratory manual, 3rd ed. Cold Spring Harbor Laboratory Press, 2001.
[7] S. Fredriksson, M. Gullberg, J. Jarvius, C. Olsson, K. Pietras, S.M. Gústafsdóttir, et al., Protein detection using proximity-dependent DNA ligation assays, Nature Biotechnology 20 (2002) 473–477.
[8] K. Lymperopoulos, R. Crawford, J.P. Torella, M. Heilemann, L.C. Hwang, S.J. Holden, et al., Single-molecule DNA biosensors for protein and ligand detection, Angewandte Chemie International Edition 49 (2010) 1316–1320.
[9] F. Jacob, J. Monod, Genetic regulatory mechanisms in the synthesis of proteins t, Journal of Molecular Biology 3 (1961) 318–356.
[10] M. Lewis, A tale of two repressors, Journal of Molecular Biology 409 (2011) 14–27.
[11] S.J. Holden, S. Uphoff, J. Hohlbein, D. Yadin, L. Le Reste, O.J. Britton, et al., Defining the limits of single-molecule FRET resolution in TIRF microscopy, Biophysical Journal 99 (2010) 3102–3111.
[12] J. Vogelsang, R. Kasper, C. Steinhauer, A reducing and oxidizing system minimizes photobleaching and blinking of fluorescent dyes, Angewandte Chemie International Edition 47 (2008) 5465–5469.
[13] G. Cowan, Statistical data analysis, Oxford University Press, 1998.
[14] W.H. Press, S.A. Teukolsky, W.T. Vetterling, B.P. Flannery, Numerical recipes, The art of scientific computing, 3rd edition, Cambridge University Press, 2007.
[15] K.L. Lange, R.J.A. Little, J.M.G. Taylor, L. Lange, M.G. Taylor, Robust statistical modeling using the t distribution, Journal of the American Statistical Association 84 (1989) 881.
[16] D.J. Peel, G.J. McLachlan, Robust mixture modelling using the t distribution, Statistics and Computing 10 (2000) 339–348.
[17] T. Heyduk, E. Heyduk, Molecular beacons for detecting DNA binding proteins, Nature Biotechnology 20 (2002) 171–176.
[18] E. Heyduk, E. Knoll, T. Heyduk, Molecular beacons for detecting DNA binding proteins: mechanism of action* 1, Analytical Biochemistry 316 (2003) 1–10.
[19] M.C. Mossing, M.T. Record, Thermodynamic origins of specificity in the lac repressor–operator interaction: adaptability in the recognition of mutant operator sites, Journal of Molecular Biology 186 (1985) 295–305.
[20] D.V. Goeddel, Binding of synthetic lactose operator DNAs to lactose repressors, Proceedings of the National Academy of Sciences 74 (1977) 3292–3296.
[21] P.A. Whitson, J.S. Olson, K.S. Matthews, Thermodynamic analysis of the lactose repressor–operator DNA interaction, Biochemistry 25 (1986) 3852–3858.
[22] A.D. Riggs, H. Suzuki, S. Bourgeois, Lac repressor–operator interaction. I. Equilibrium studies, Journal of Molecular Biology 48 (1970) 67–83.
[23] A.D. Riggs, S. Bourgeois, M. Cohn, The lac represser–operator interaction* 1,* 2: III. Kinetic studies, Journal of Molecular Biology 53 (1970) 401–417.
[24] J. SantaLucia, A unified view of polymer, dumbbell, and oligonucleotide DNA nearest-neighbor thermodynamics, Proceedings of the National Academy of Sciences 95 (1998) 1460–1465.
[25] W. Trabesinger, B. Hecht, U.P. Wild, G.J. Schütz, H. Schindler, T. Schmidt, Statistical analysis of single-molecule colocalization assays, Analytical Chemistry 73 (2001) 1100–1105.
[26] M.J. Levene, J. Korlach, S.W. Turner, M. Foquet, H.G. Craighead, W.W. Webb, Zero-mode waveguides for single-molecule analysis at high concentrations, Science 299 (2003) 682–686.
[27] Z. Wunderlich, L.A. Mirny, Different gene regulation strategies revealed by analysis of binding motifs, Trends in Genetics (2009) 1–7.
[28] M. John, R. Leppik, S.J. Busch, M. Granger-Schnarr, M. Schnarr, DNA binding of Jun and Fos bZip domains: homodimers and heterodimers induce a DNA conformational change in solution, Nucleic Acids Research 24 (1996) 4487.
[29] C.M. Klinge, Estrogen receptor interaction with estrogen response elements, Nucleic Acids Research 29 (2001) 2905–2919.
[30] B. Sclavi, S. Woodson, M. Sullivan, M.R. Chance, M. Brenowitz, Time-resolved synchrotron X-ray, Journal of Molecular Biology 266 (1997) 144–159.
[31] M. Hsieh, M. Brenowitz, Comparison of the DNA association kinetics of the lac repressor tetramer, its dimeric mutant laci adi, and the native dimeric gal repressor *, The Journal of Biological Chemistry 272 (1997) 22092–22096.
[32] M.M. Levandoski, O.V. Tsodikov, D.E. Frank, S.E. Melcher, R.M. Saecker, T.M. Record Jr., Cooperative and anticooperative effects in binding of the first and second plasmid osymoperators to a laci tetramer: evidence for contributions of non-operator dna binding by wrapping and looping, Journal of Molecular Biology 260 (1996) 697–717.
[33] K.M. Vossen, D.F. Stickle, M.G. Fried, The mechanism of CAP-lac repressor binding cooperativity at the *E. coli* lactose promoter, Journal of Molecular Biology 255 (1996) 44–54.